International Journal of Minerals, Metallurgy and Materials
Volume 19, Number 2, Feb 2012, Page 165
DOI: 10.1007/s12613-012-0533-2

Kinetics and mechanism of titanium hydride powder and aluminum melt reaction

Ali Rasooli[1)], *Mehdi Divandari*[1)], *Hamid Reza Shahverdi*[2)], *and Mohammad Ali Boutorabi*[1)]

1) School of Metallurgy and Materials Engineering, Member of Center of Excellence for Advanced Material and Processing (CEAMP), Iran University of Science and Technology, Tehran 16844, Iran

2) Department of Materials, Faculty of Engineering, Tarbiat Modaress University, Tehran 14115-143, Iran

(Received: 18 January 2011; revised: 5 February 2011; accepted: 14 February 2011)

Abstract: Based on the measurement of the released hydrogen gas pressure (P_{H_2}), the reaction kinetics between TiH_2 powder and pure aluminum melt was studied at various temperatures. After cooling the samples, the interface of TiH_2 powder and aluminum melt was studied. The results show that the P_{H_2} -time curves have three regions; in the first and second regions, the rate of reaction conforms zero and one order, respectively; in the third region, the hydrogen gas pressure remains constant and the rate of reaction reaches zero. The main factors that control the rate of reaction in the first and second regions are the penetration of hydrogen atoms in the titanium lattice and the chemical reaction between molten aluminum and titanium, respectively. According to the main factors that control the rate of reaction, three temperature ranges are considered for the reaction mechanism: (a) 700-750°C, (b) 750-800°C, and (c) 800-1000°C. In the first temperature range, the reaction is mostly under the control of chemical reaction; at the temperature range of 750 to 800°C, the reaction is controlled by the diffusion and chemical reaction; at the third temperature range (800-1000°C), the dominant controlling mechanism is diffusion.

Keywords: titanium hydride; aluminum; reaction kinetics; reaction rate constants

1. Introduction

TiH_2 powder is used as a bubble agent in the liquid foaming process for producing aluminum metallic foams [1-4], and the bubble flow is one of the most important phenomena, which limits the liquid foaming process [5]. In this process, the precise control of bubble growth in melt results in the foams of regular structures [2, 6]. Bubble growth depends on gas production in melt due to the reaction between TiH_2 powder and aluminum melt [2, 7-8]. This reaction is influenced by different factors, such as hydride phase decomposition, the penetration of hydrogen in titanium lattice, and various generated hydride phases on the surface of powders [9].

Although several studies have been done on the TiH_2 decomposition [10-17], there are few reports about the foaming by means of the bubble producer [5]. Compared to the powder method, less research has been done in the liquid foaming approach [2-6]. Duarte and Banhart have studied the kinetics process of foam decomposition in powder foaming by measuring the expansion rate of foam [18]. TiH_2 decomposition is conducted by heating to high temperatures gradually (*e.g.*, melting point of alloys), and the results are used in the kinetics analysis. While in the liquid foaming approach, the powder is directly added to the melt, reacts with the melt, and produces hydrogen gas. Therefore, the study of kinetics reaction of TiH_2 powder with the melted aluminum is very important for determining and controlling the conditions of foaming processes.

Regarding the large amounts of hydrogen gas production in the reaction between TiH_2 powder and aluminum melt, the alteration of released hydrogen gas pressure can be considered as one of the main factors of bubble growth in melt. In this research, the kinetics of reaction between TiH_2 powder and aluminum melt was studied by the direct measurement of released hydrogen gas pressure. Following the solidification of samples, the interface of TiH_2 powder and melt was studied to determine the mechanism of reaction.

Corresponding author: Ali Rasooli E-mail: ali_rasooli@iust.ac.ir

2. Experimental

The as-received TiH_2 powder (Merck, 98% purity), with the particle size ranging from 2 to 12 μm, was characterized by scanning electron microscopy (SEM, Philips Model XL30, Netherlands) for its morphology, energy-dispersive spectroscopy (EDS) for its element content, X-ray diffraction (XRD, Philips Model PW3710, Netherlands) for its phase, and a laser particle sizer (analysette 22, Germany) for its size distribution. The pure commercial aluminum bar (99.91% purity) was used as a raw material. The chemical composition of the aluminum bar is shown in Table 1. The direct measurement setup of released hydrogen gas pressure is illustrated in Fig. 1.

In this system, 400-mm pipe AISI 304 stainless steel for the closed-end pipe (Fig. 2(a)), 480-mm pipe AISI 304 stainless steel for the internal pipe (Fig. 2(b)), and 350-mm pipe AISI 321 stainless steel are used to make the pod (Fig. 2(c)); also, the 750-mm silicon hose, fitting to the pipe, is used.

Table 1. Chemical composition of the pure commercial aluminum rod bar **wt%**

Al	Si	Fe	Cu	Zn
99.70	0.12	0.12	0.04	0.01

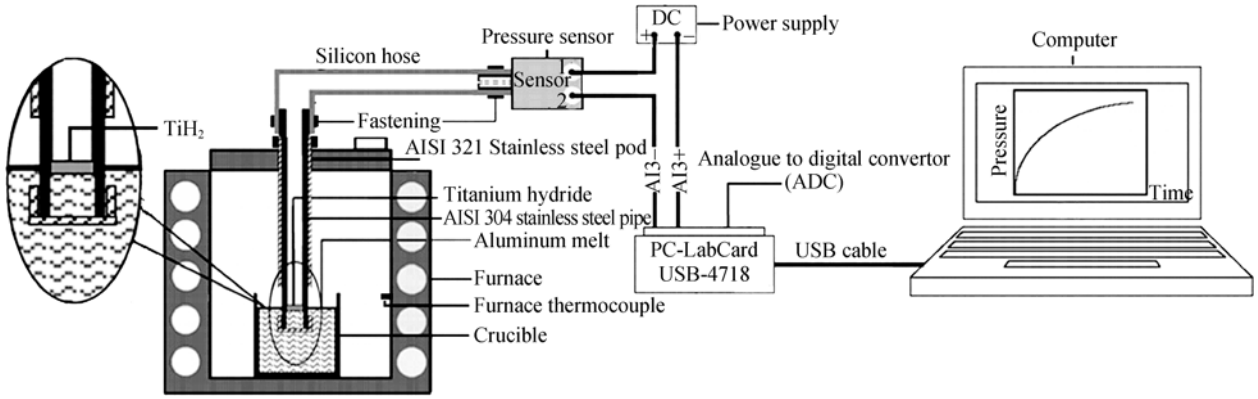

Fig. 1. Schematic setup for the online measurement of gas pressure.

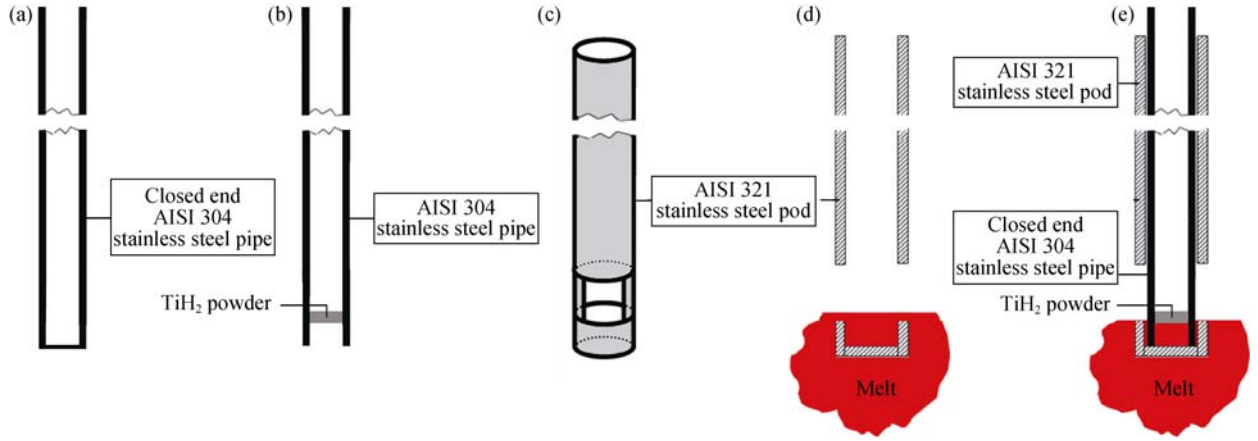

Fig. 2. Closed-end pipe (a), TiH_2 powder within pipe (b), pod (c), pod into the melt (d), and way of placing the stainless steel pod and pipe containing powder into the melt (e).

At the first stage, after installation of the setup as shown in Fig. 1 and melting the aluminum bar, a closed-end AISI 304 stainless steel pipe (about 1 to 2 cm as shown in Fig. 2(a)) without TiH_2 powder is entered into the melt, and the pressure of warm air (P_{air}), which exists inside the pipe, is measured at various temperatures. In the second stage, 0.1 g TiH_2 powder is put into an open-ended pipe, made of AISI 304 stainless steel (Fig. 2(b)). In the third stage, about 2 to 3 cm of the pod is entered to the melt (Fig. 2(d)); then, the same procedure is done for the pipe, containing TiH_2 powder; finally, the pressure of gas within the pipe (P_{total}) is determined at various temperatures (Fig. 2(e)). According to Eq. (1), the hydrogen gas pressure (P_{H_2}) at various temperatures is calculated as

$$P_{H_2} = P_{total} - P_{air} \quad (1)$$

After constancy of hydrogen gas pressure, the pipe and pod existed in the melt until the melt reacted with the powder solidified. When the reaction between the powder and melt was done, the microstructure of the interface between the powder and melt was investigated by SEM. Also, the powders were characterized by EDS and XRD.

3. Results and discussion

3.1. Characteristics of titanium hydride powder characteristics

Fig. 3 shows the particle size distribution and the SEM image of TiH_2 powder. The mean size of TiH_2 powder is about 8 to 12 μm as shown in Fig. 3(a), and the corresponding SEM image is shown in Fig. 3(b).

Fig. 4 shows the chemical analysis of the TiH_2 powder by EDS and XRD, respectively. According to EDS, titanium is the only detectable element and no major impurity is revealed. The XRD pattern indicates that the state of hydrogenation is $TiH_{1.924}$.

3.2. Kinetics analysis

The P_{H_2} -time curves at various temperatures are shown in Fig. 5. The curves can be divided into three regions. In the first region, the pressure increases linearly; while in the second region, it shows a parabolic manner; in the third region, it remains constant. The maximum hydrogen pressure and the time needed to reach the maximum pressure for each region are shown in Table 2.

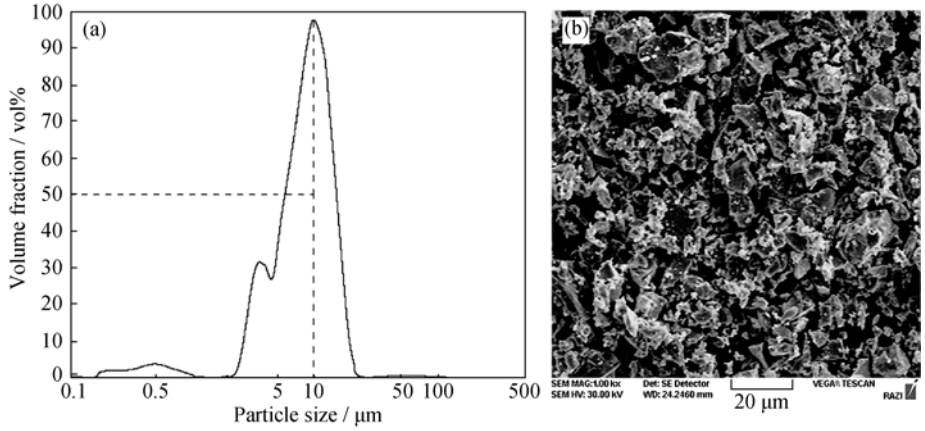

Fig. 3. Particle size distribution of as-received TiH_2 powder (a) and the corresponding SEM image (b).

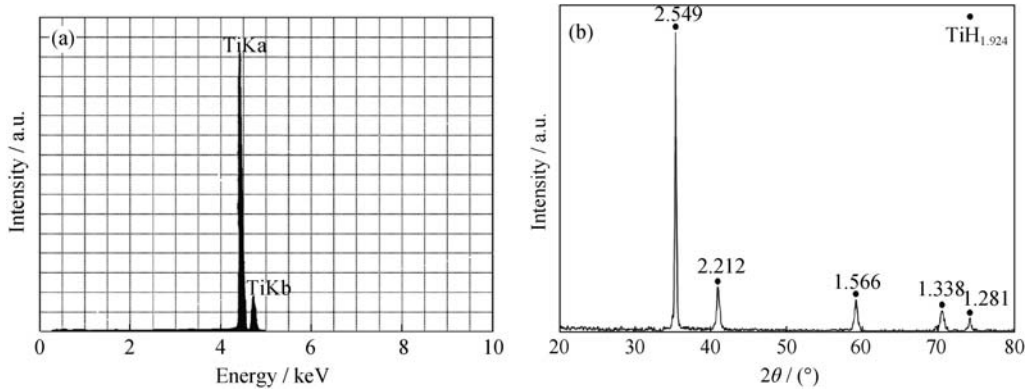

Fig. 4. EDAX spectrum (a) and XRD pattern (b) of TiH_2 powder.

It can be seen from Table 2 that, in the first and second regions, the maximum pressure of hydrogen rises with the melt temperature increasing, while the time range of the second region reduces and the beginning time of the second region increases. In the third region, the hydrogen gas pressure remains constant, which is almost equal to the maximum pressure of the second region. Therefore, considering the maximum pressure difference between the first and second regions at various temperatures, it can be seen that most of hydrogen is produced in the first region, which means that most of the reaction between TiH_2 powder and the melt is performed in the first region.

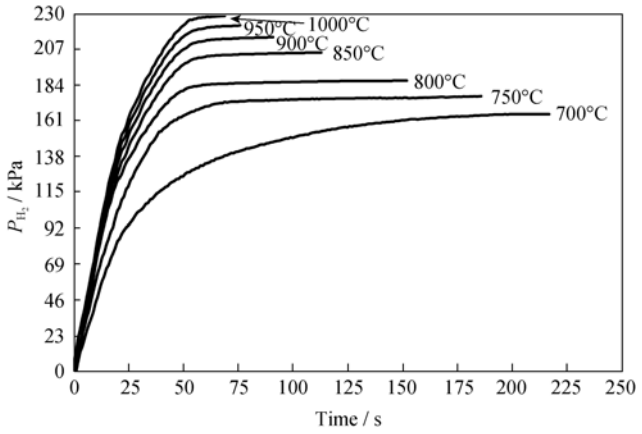

Fig. 5. P_{H_2} **-time curves at various temperatures.**

The study of P_{H_2} -time curves in the first region is shown in Fig. 6. It can be seen that, when the temperature is higher than 750°C, the hydrogen gas pressure (P_{H_2}) increases by two different slopes. Because the variations of pressure are linear, the reaction rate of TiH_2 powder and aluminum melt is at zero order. Therefore, the linear slope of P_{H_2} -time curves is equal to the reaction rate constant, and the reaction rate constants are shown in Table 3. According to Table 3, when the temperature rises, the reaction rate constant increases. Therefore, the reaction rate increases and much more amounts of hydrogen are released. The second rate constant is smaller than the first one, indicating that the rate of hydrogen emission from titanium hydride decreases.

Table 2. Maximum hydrogen gas pressure and time for each region at various temperatures

Temperature / °C	First region		Second region		Third region	
	Max. pressure / kPa	Reaching time / s	Max. pressure / kPa	Reaching time / s	Max. pressure / kPa	Reaching time / s
700	87	0-20	165	21-190	~166	>190
750	133	0-30	174	31-70	~174	>70
800	154	0-35	185	35-59	~185	>59
850	182	0-40	203	40-56	~203	>56
900	195	0-42	213	42-54	~213	>54
950	210	0-44	225	44-52	~221	>52
1000	224	0-48	228	48-50	~228	>50

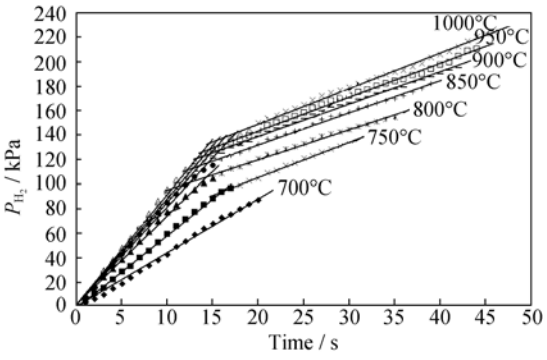

Fig. 6. P_{H_2} **-time curves at various temperatures in the first region.**

In Fig. 5, the P_{H_2} -time curves show a parabolic manner in the second region. By a derivative method, the equation order of reaction between TiH_2 powder and aluminum melt is determined as one as shown in Fig. 7. The reaction rate constants are determined at various temperatures in Table 4.

Table 3. Reaction rate constants at various temperatures in the first region

Temperature / °C	Reaction rate constant in the first region / ($kPa \cdot s^{-1}$)	
	First rate constant	Second rate constant
700	4.603	—
750	5.936	2.867
800	7.253	2.449
850	7.978	2.632
900	8.362	2.656
950	8.652	2.777
1000	8.999	2.910

Based on the Arrhenius equation (Eq. (2)), the activation energies in the first region for the first and second stages are determined as approximately 22 and 9 kJ/mol, respectively. In the second region, the activation energy is nearly 105 kJ/mol as shown in Fig. 8.

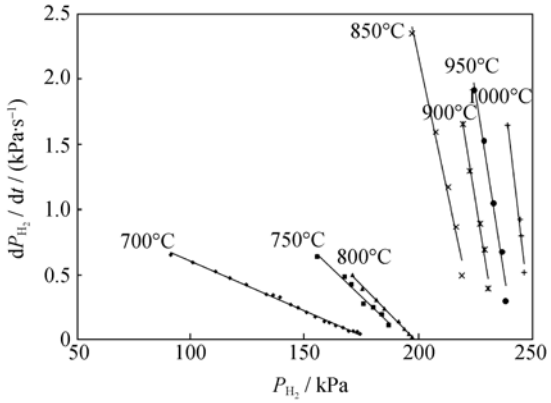

Fig. 7. Variation of dP_{H_2}/dt *vs.* P_{H_2} at various temperatures in the second region.

Table 4. Reaction rate constants at various temperatures in the second region

Temperature /°C	Rate constant / s^{-1}
700	–0.0076
750	–0.0167
800	–0.0178
850	–0.0814
900	–0.1014
950	–0.1112
1000	–0.1481

$$K = A \cdot \exp\left(-\frac{Q}{R \cdot T}\right) \quad (2)$$

where K is the rate constant, A the frequency factor, Q the activation energy, R the gas constants, and T the absolute temperature.

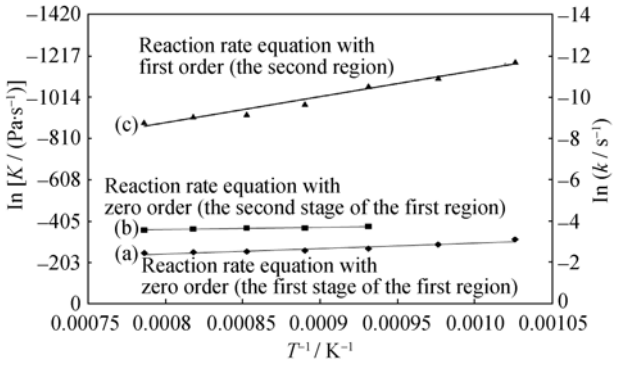

Fig. 8. Arrhenius plots: (a) the first stage of the first region; (b) the second stage of the first region; (c) the second region.

3.3. Powder and melt interface analysis

Fig. 9 shows the SEM images of TiH_2 powder particles in the melt after solidification at various temperatures, including 700, 750, 800, 850, 900, 950, and 1000°C. Fig. 10 shows the EDAX analysis of points labeled as A, B, and C at SEM images in Fig. 9. The XRD patterns of samples are shown in Fig. 11.

According to the SEM images, EDAX analysis, and XRD patterns, it can be concluded that, when the TiH_2 powder reacts with the aluminum melt, $TiAl_3$ is formed. In Fig. 9(a), a continuous layer of $TiAl_3$ with almost 3 μm in thickness is formed on the powder particle surface at 700°C. A 1.5-μm thickness continuous layer of $TiAl_3$ is seen on the powder particle surface at 750°C. The $TiAl_3$ layer surface is not smooth and seems to be collapsed. Meanwhile, the powder particle surface is like a half-collapsed material as shown in Fig. 9(b).

In Fig. 9(c), the $TiAl_3$ layer formed on the powder particle surface is nearly scattered and seems to separate from the surface of powder particles. There are some holes within the powder particles, which seem to be the result of gas production in the TiH_2 powder bulk. Above 800°C, the $TiAl_3$ layer formed on the powder particle surface is scattered and separates from the powder particle surface. At temperatures between 850 and 1000°C, the surface of powder particles shows a scattered mode, which is due to the production of a large amount of hydrogen gas within the powder body as shown in Figs. 9(d)-(g).

3.4. Kinetics and reaction mechanism

Regarding the gas production of metal hydride [9] based on the Castro-Meyer model [19] and the shrinking core model [20], it seems that the mechanism is controlled by three factors: (a) external diffusion (mass transfer in the melt phase); (b) chemical reaction (the reaction of titanium and melt); (c) internal diffusion (hydrogen atom diffusion within the titanium lattice and $TiAl_3$ layer). The following factors have been considered in the research: (1) the smaller volume of melt (nearly 0.5 cm^3) in contact with a large amount of TiH_2 powder (0.1 g) in comparison with the liquid foaming (the amount of the powder is 1.6wt% melt in this method [4]); (2) the smaller size of TiH_2 powder particles (almost between 2 and 12 μm); (3) the higher temperature of the melt compared to the internal transformation temperature of TiH_2 powder [10-13, 16] (about 530°C in the first transformation and the next one is about 640°C [21]); (4) increasing the hydrogen gas pressure in a short time.

It seems that factors such as gas transfer in the melt and gas phases, the surface adsorption and desorption of hydrogen atoms, and the conversion of hydrogen atoms to hydrogen molecules are quick phenomena [22]. Therefore, the

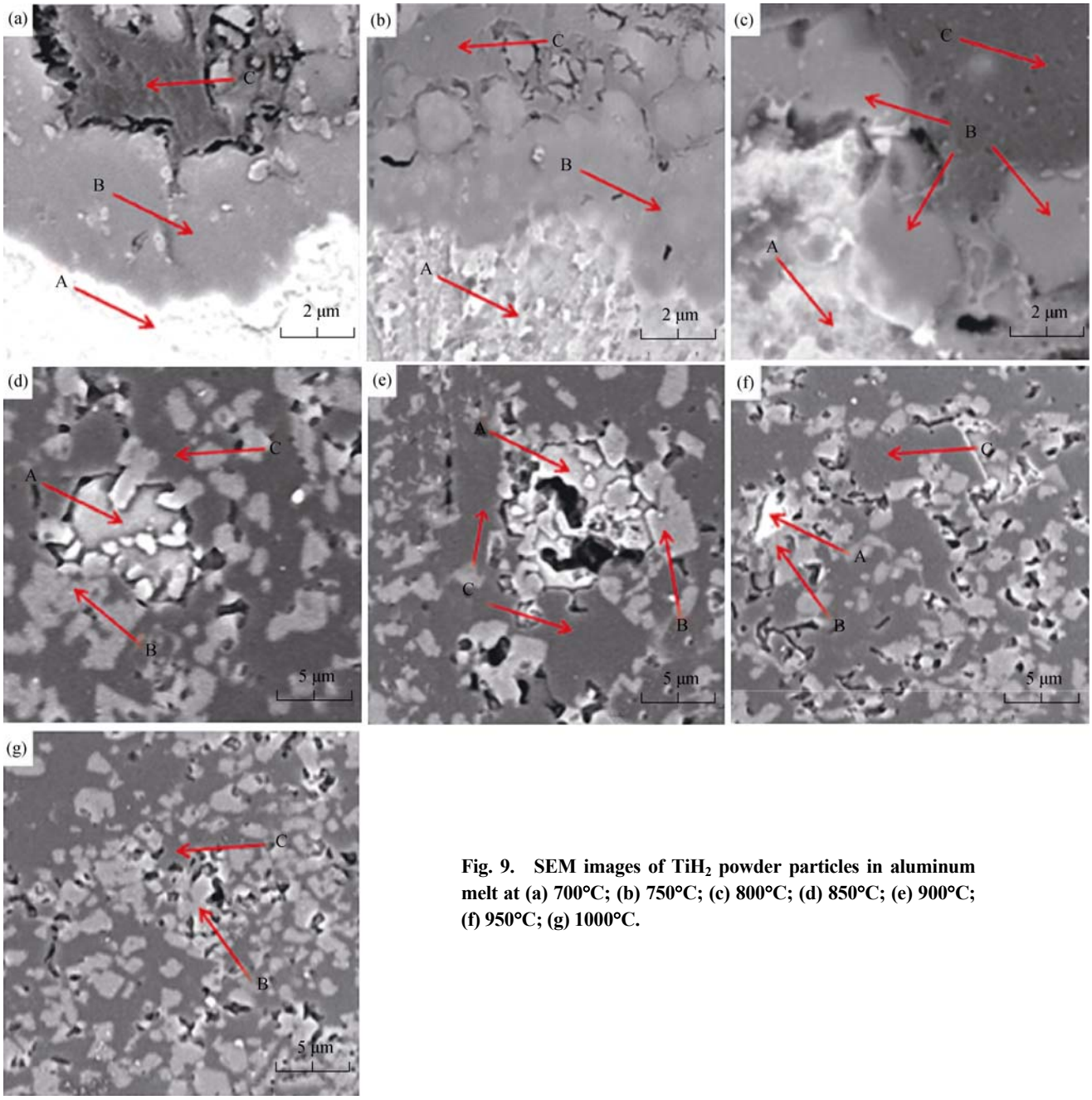

Fig. 9. SEM images of TiH_2 powder particles in aluminum melt at (a) 700°C; (b) 750°C; (c) 800°C; (d) 850°C; (e) 900°C; (f) 950°C; (g) 1000°C.

main parameters in kinetics are the internal diffusion and chemical reaction. Various reports [10-13, 16, 21] on the hydrogen emission from TiH_2 in air and argon gas, the oxidation of TiH_2 [10-13], and the higher temperature of aluminum melt in this work, compared to the internal transformation temperatures of TiH_2, [21] show that hydrogen atoms start to exit from the TiH_2 lattice before reaction with aluminum melt. Therefore, the reaction of the powder and melt is primarily controlled by the diffusion of hydrogen atoms into the titanium lattice. The two regions are distinguished as the following: (1) in the first region, the determined activation energy in the first stage (22 kJ/mol) is related to the hydrogen emission from TiH_2 powder ($TiH_2 \rightarrow TiH_x$), and the second stage (9 kJ/mol) is as a result of transformations of TiH_x to α-Ti; (2) in the second region, the activation energy is calculated as 105 kJ/mol, which is possibly the reaction of Ti and aluminum melt, nearly similar to the report by Vyazovkin (97 kJ/mol) and Wang (109 kJ/mol) [23-24].

As shown in Figs. 10-11, when the content of Ti exceeds 0.15wt% and the temperature is above 665°C [25], $TiAl_3$ forms. SEM images in Fig. 9 show that, as the temperature

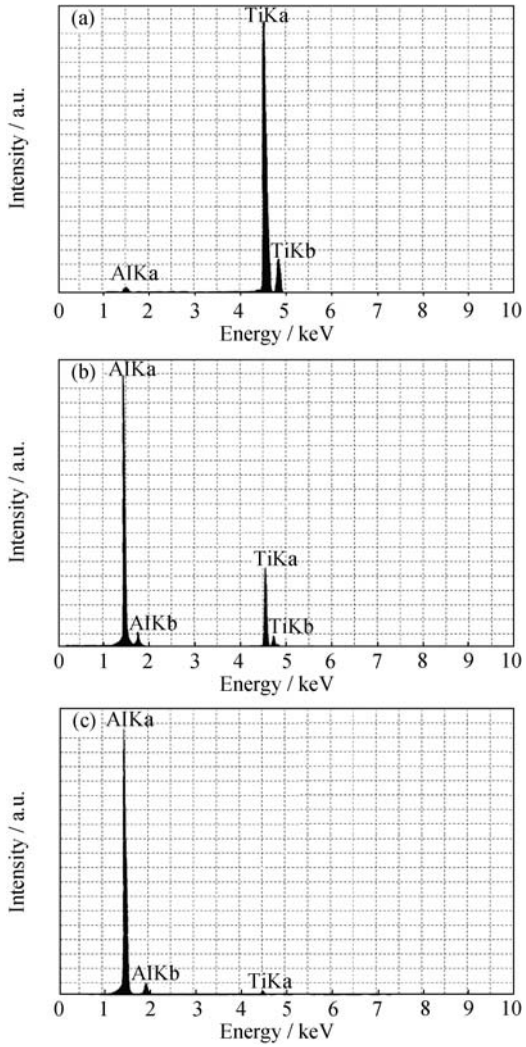

Fig. 10. EDAX analysis of points A, B, and C in Fig. 8: (a) A point; (b) B point; (c) C point.

increases, the $TiAl_3$ layer on the powder particle scatters following by scattering of the remaining part of the particle. It means that the $TiAl_3$ layer cannot prevent the powder to be contacted with the melt; therefore, the chemical reaction speeds up. As a result, the internal diffusion, not the chemical reaction, acts as the rate controlling factor.

As shown in Fig. 5, when the temperature increases, the first region extends and the second region contracts. This indicates that the dominant mechanism changes from the chemical reaction to the internal diffusion. At 700°C, when the thickness of the $TiAl_3$ continuous layer increases, the diffusion of hydrogen atoms within this layer decreases. The rate of hydrogen production gradually decreases and finally reaches zero. Consequently, the chemical reaction is the controlling factor. At 750°C, as a result of $TiAl_3$ scattering, the diffusion of hydrogen atoms through the $TiAl_3$ layer increases. Therefore, the rate of chemical reaction increases.

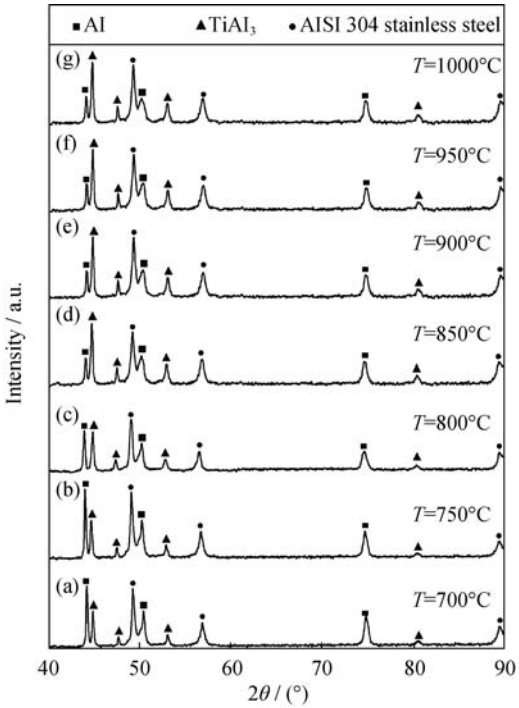

Fig. 11. XRD patterns of samples after solidification at: (a) 700°C; (b) 750°C; (c) 800°C; (d) 850°C; (e) 900°C; (f) 950°C; (g) 1000°C.

In this case, the rate of reaction is controlled by both the chemical reaction and the internal diffusion parameters. Above 800°C, the $TiAl_3$ layer becomes scattered and Ti contacts with melt. In this temperature range, the chemical reaction occurs very fast and cannot control the rate of reaction. Thus, the dominant controller of rate is the internal diffusion. It seems that, at temperatures higher than 850°C, the hydrogen production is the result of heat decomposition of TiH_2 powder.

Based on the above results, it seems that the mechanism of hydrogen release is as a result of TiH_2 powder interaction with the pure aluminum melt, and it can be categorized in three temperature ranges: 700-750°C, 750-800°C, and 800-1000°C. At 700-750°C, the dominant factor that controls the rate of reaction is mostly the chemical reaction. At 750-800°C, it is controlled by the internal diffusion and the chemical reaction. At 800-1000°C, the dominant controlling mechanism is diffusion.

4. Conclusions

(1) The rate of reaction between TiH_2 powder and aluminum melt conforms to zero and first order in the first and second regions, respectively.

(2) The reaction mechanism between TiH_2 powder and aluminum melt is controlled by hydrogen atom diffusion

within titanium lattices and the reaction of titanium and aluminum melt.

(3) The process of diffusion occurs through two stages, and the activation energies of the first and second transformations are determined as about 22 and 9 kJ/mol, respectively.

(4) During the reaction of TiH_2 powder and aluminum melt, the $TiAl_3$ layer forms on the powder particle surface. The activation energy is determined as about 105 kJ/mol.

(5) At the temperature ranges of 700 to 750°C, 750 to 800°C, and 800 to 1000°C, the mechanism of reaction is controlled by chemical reactions, diffusion and chemical reactions, and diffusion, respectively. At temperatures higher than 850°C, the thermal decomposition of TiH_2 powder occurs.

References

[1] J. Banhart and D. Weaire, On the road again: metal foams find favor, *Phys. Today*, 55(2002), p.37.

[2] J. Banhart, Aluminum Foams: On the Road to real Applications, *MRS Bull.*, 28(2003), No.4, p.290.

[3] J. Banhart, Manufacture, characterisation and application of cellular metals and metal foams, *Prog. Mater. Sci.*, 46(2001), p.559.

[4] T. Miyoshi, M. Itoh, S. Akiyama, and A. Kitahara, ALPORAS aluminum foam: production process, properties, and applications, *Adv. Eng. Mater.* 2(2000), No.4, p.179.

[5] J. Banhart, Metal foams: production and stability, *Adv. Eng. Mater.*, 8(2006), No.9, p.871.

[6] A. Haibel, A. Rack, and J. Banhart, Why are metal foams stable? *Appl. Phys. Lett.*, 89(2006), art. No.154102.

[7] D.H. Yang and B.Y. Hur, The relationship between thermal decomposition properties of titanium hydride and the Al alloy melt foaming process, *Mater. Letter.*, 60(2006), p.3635.

[8] D.H. Yang, B.Y. Hur, D.P. He, and S.R. Yang, Effect of decomposition properties of titanium hydride on the foaming process and pore structures of Al alloy melt foam, *Mater. Sci. Eng. A*, 445-446(2007), p.415.

[9] I.E. Gabis, A.P. Voit, E.A. Evard, *et al.*, Kinetics of hydrogen desorption from the powders of metals hydrides, *J. Alloys Compd.*, 404-406(2005), p.312.

[10] F. Von Zeppelin, M. Hirscher, H. Stanzick, and J. Banhart, Desorption of hydrogen from blowing agents used for foaming metals, *Compos. Sci. Technol.*, 63(2003), p.2293

[11] V. Bhosle, E.G. Baburaj, M. Miranova, and K. Salama, Dehydrogenation of TiH_2, *Mater. Sci. Eng. A*, 356(2003), p.190.

[12] A.R. Kennedy and V.H. Lopez, The decomposition behavior of as-received and oxidized TiH_2 foaming-agent powder, *Mater. Sci. Eng. A*, 357(2003), p.258.

[13] H.R.Z. Sandim, B.V. Morante, and P.A. Suzuki, Kinetics of thermal decomposition of titanium hydride powder using in situ high-temperature X-ray diffraction (HTXRD), *Mater. Res.*, 8(2005), No.3, p.293.

[14] B. Tsuchiya, M. Teshigawara, S. Nagata, *et al.*, Hydrogen analyses of titanium hydride by ERD and NRG Methods, *Nuclear Instrum. Methods Phys. Res. B*, 190(2002), p.699.

[15] A.R. Kennedy, The effect of TiH_2 heat treatment on gas release and foaming in Al-TiH_2 performs, *Scripta Mater.*, 47(2002), p.763.

[16] B. Matijasevic-Lux, J. Banhart, S. Fiechter, *et al.*, Modification of titanium hydride for improved aluminium foam manufacture, *Acta Mater.*, 54(2006), p.1887.

[17] B. Tsuchiya, S. Nagata, N. Ohtsu, K. Toh, and T. Shikama, Thermal desorption of hydrogen at the titanium hydride-oxide interface, *Jpn. Inst. Met.*, 46(2005), p.196.

[18] I. Duarte and J. Banhart, A study of aluminium foam formation kinetics and microstructure, *Acta Mater.*, 48(2000), p.2349.

[19] F.J. Castro and G. Meyer, Thermal desorption spectroscopy (TDS) method for hydrogen desorption characterization (I): theoretical aspects, *J. Alloys Compd.*, 330(2002), p.59.

[20] V.R. Subramanian, H.J. Ploehn, and R.E White, Shrinking core model for the discharge of a metal hydride electrode, *J. Electrochem. Soc.*, 147(2000), p.2868.

[21] A. Rasooli, M. Divandari, H.R. Shahverdi, and M.A Boutorabi, Effect of ambient atmosphere and the rate of heating on the behavior of thermal decomposition titanium hydride (TiH_2) powder, *J. Metall. Mater. Eng.*, 21(2009), No.1, p.58.

[22] Kh.A. Sadrnezhaad, *Kinetic Processes in Materials Engineering and Metallurgy*, Amir Kabir Publication Organization, Tehran, 1994, p.85.

[23] S. Vyazovkin, Conversion dependence of activation energy for model DSC curves of consecutive reactions, *Thermochim. Acta*, 236(1994), p.1.

[24] T. Wang and J.S. Zhang, Thermoanalytical and metallographical investigations on the synthesis of $TiAl_3$ from elementary powders, *Mater. Chem. Phys.*, 99(2006), p.20.

[25] M. Sujata, S. Bhargava, and S. Sangal, On the formation of $TiAl_3$ during reaction between solid Ti and liquid Al, *J. Mater. Sci. Lett.*, 16(1997), p.1175.